Experimental Assessment of the Effect of Print Orientation on the Geometrical Accuracy of Microfeatures in Multi-Material 3D Inkjet Printing

Karin J. Chen[1,2,*], Ahmed Elkaseer[3], Veit Hagenmeyer[1], Steffen G. Scholz[1,2]

[1] *Institute for Automation and Applied Informatics, Karlsruhe Institute of Technology, Hermann-von-Helmholtz-Platz 1, 76344 Eggenstein-Leopoldshafen, Germany*
[2] *Karlsruhe Nano Micro Facility (KNMFi), Karlsruhe Institute of Technology, Hermann-von-Helmholtz-Platz 1, 76344 Eggenstein-Leopoldshafen, Germany*
[3] *Department of Mechanical Engineering, Faculty of Engineering, The British University in Egypt, El-Sherouk City 11837, Egypt*
*Corresponding author: Karin J. Chen, *karin.chen@kit.edu*

Abstract

3D inkjet printing is an additive manufacturing technology that allows for the printing of multi-material features in the micrometre range with high accuracy, utilizing multiple printheads at the same time. In this study, two UV-curable materials, i.e. build material and water-soluble support material, are printed to create a specimen with overall sizes of up to 8x8x8 mm³, containing microcolumns and walls with widths ranging from 50 µm to 500 µm, equivalent to an aspect ratio between 0.01 and 0.5 (width/height). The objective of this study is to investigate qualitatively and to understand how the placement orientation of the object on the print platform affects the geometrical accuracy of the printed microfeatures. This study reveals that horizontal edges are most accurate when the specimen is rotated either around the print direction or the printhead axis by 45°. Conversely, horizontal edges that are parallel to the printing plane all exhibit a convex shape, most likely induced by the differing droplet coalescence behaviour between support/build material and build/build material interactions. The columns of consistent diameter (0.5 mm) and varying height (1, 2, and 3 mm) are printed successfully, although some are tilted in arbitrary directions. This tilting could be due to droplet variation between nozzles, skewed trajectories of printed droplets, or differences in layer height between materials. The majority of the printed thin walls, which are 50 µm wide, have collapsed, in particular the vertical ones.

Keywords: 3D inkjet printing, print orientation, microfeatures, multi-material printing, additive manufacturing

1. Introduction

3D inkjet printing (3D-IJ), also known as material jetting, is an additive manufacturing (AM) technology that utilizes piezo-based printheads to generate thousands of droplets, which coalesce and form a layer upon deposition on the substrate. By printing layer by layer, a 3D printed object is created. 3D-IJ is considered a high-accuracy and high-precision AM technology, allowing features in the micrometer range to be printed. Additionally, it can simultaneously process multiple materials during the printing process by utilizing multiple printheads [1]. State-of-the-art reports highlight numerous advanced multi-material applications with 3D-IJ, such as the printing of electronic circuits [2], actuators [3], pharmaceuticals with multiple active substances [4], soft grippers [5] or functionally graded structures [6].

3D-IJ often necessitates the printing of at least two materials, as the designed object frequently requires both build material and support material [7]. Support material is used for the support of overhanging structures or for (thin) vertical structures, limiting the spreading of the droplets until they solidify [8]. Support material can also be used to modify the surface quality [9].

Several studies on multi-material 3D-IJ printing have reported the correlation between mechanical properties and interface orientation between two materials [10, 11]. Further research studies have investigated the relationship between dimensional accuracy and print orientation [12, 13]. Existing studies on multi-material 3D printing utilize commercial printers with predefined printing settings according to the materials used, optimizing parameters to guarantee consistent droplet properties. These settings, provided by the manufacturers, eliminate issues of layer variation but do not allow systematic studies on the correlation between interface properties and droplet and material properties. Furthermore, the dimensions of the assessed specimens range from a few dozen micrometers [14] to several dozen millimeters. However, Silva et al. (2021) concluded that only cubes with an edge length greater than 212 µm could be printed [14].

Considering the capability of 3D-IJ to manufacture high-precision objects with multiple materials, there is a gap in the state-of-the-art regarding the impact of print part orientation on geometrical accuracy for microfeatures. This present study focuses on the geometrical deviation of specimens with microfeatures and aims to determine the relevant factors to be considered in 3D-IJ in order to achieve high-accuracy print results.

2. Materials and Methods

Fig. 1 summarizes the materials and methods used in this study. The printed specimen consists of various columns and walls with different widths and heights, covering an aspect ratio of 0.01 to 0.5. Each side possesses either a group of four columns of the same length (1, 2, or 3 mm) and consistent width (0.5 mm) or a group of six thin walls of the same length (1, 2, or 3 mm) and varying widths (0.05, 0.1, 0.2, 0.3, 0.4, and 0.5 mm) (Fig. 1a).

This test specimen is printed at 13 different

positions and orientations on the printing platform of the 3D-IJ printer njet3D by Notion Systems, Germany (Fig. 1d).

The assigned name of each specimen corresponds to the geographic location viewed from the operator. The specimens at positions North1 (N1), East1 (E1), South1 (S1), West1 (W1), and Centre (C) are flipped by 90°, meaning that they are placed on different sides of the test specimen. The specimens at Northeast (NE), Southeast (SE), Southwest (SW), and Northwest (NW) are rotated around the build direction axis (BD) by 45°, and those placed at the outer areas, namely North2 (N2) and South2 (S2), are rotated around the printhead axis (PH) by 45°, while East2 (E2) and West2 (W2) are rotated around the print direction axis (PD) by 45° (Fig. 1b). These 13 specimens are assembled into an assembly CAD model, exported to an STL file, and then sliced into 140 layers for each printhead/material using the open-source slicer 3Dslicer (Fig. 1c).

Two UV-curable materials from BASF are used to generate the test specimens: support material SPJ1071 and build material EPJ2100 (Fig. 1e). The average droplet volume ejected by the printhead filled with build material (printhead 1) is 19.89 pl ± 3 pl, while the droplet volume of printhead 0 filled with support material is 21.45 pl ± 0.5 pl. Both materials are cured by a UV-LED source at a wavelength of 395 nm. The printing temperature is 62°C for the build material and 50°C for the support material. This temperature is necessary to ensure a viscosity that allows droplet ejection with the printhead Xaar 1003. The materials are kept in motion during the printing process by a MIDAS recirculation system. The distance between the nozzle plate and the printing plane is 800 µm.

The same waveform is applied to both printheads. However, due to the different physical properties of the two inks, the resulting droplet volumes are substantially different, necessitating an adjustment of the layer height for both materials to achieve the same value. According to Elkaseer et al. (2023) [15], the parameters that can be tuned for adjusting the layer height include grayscale level, coverage percentage, and resolution. The print resolution for both materials/printheads is kept at 1800 dpi since a different print resolution would not be processable by the printer. A UV-curing intensity of 50% is applied to the printed layer, and bidirectional curing is used in the printing process.

The printhead allows up to eight grayscale levels to be set. Grayscale printing describes the variation of the ejected droplet by applying a different waveform. Printhead 1 with build material is set to grayscale level 4, while printhead 0 with support material prints at grayscale level 2, although still producing larger droplets than printhead 1. Thus, to achieve similar layer heights, the grayscale printing of printhead 0 is combined with a dithering of the sliced image. Thirty-five percentage of the pixels required to reach full coverage for the support material are removed with a random algorithm for each layer. Under these conditions, the resulting average layer height for both materials is approximately 70 µm.

Once the printing process is completed, the support material is dissolved in deionized water for 6 hours while keeping the water in motion on a magnetic stirrer (Fig. 1g). The motion supplies fresh water around the specimen, thus avoiding saturated regions of dissolved support material in the proximity of the printed specimen.

The specimens are recorded under the optical microscope Keyence VHX7000 (Fig. 1i) and based on the images, the geometrical accuracy is evaluated with regards to three aspects. First, the quality of the top horizontal edge and the vertical edge is examined, followed by the geometrical accuracy of the columns and thin walls. Only the planes spanned by the printhead axis and the build direction (PH/BD) and the print direction and the build direction (PD/BD) (Fig. 1j) are investigated in this study.

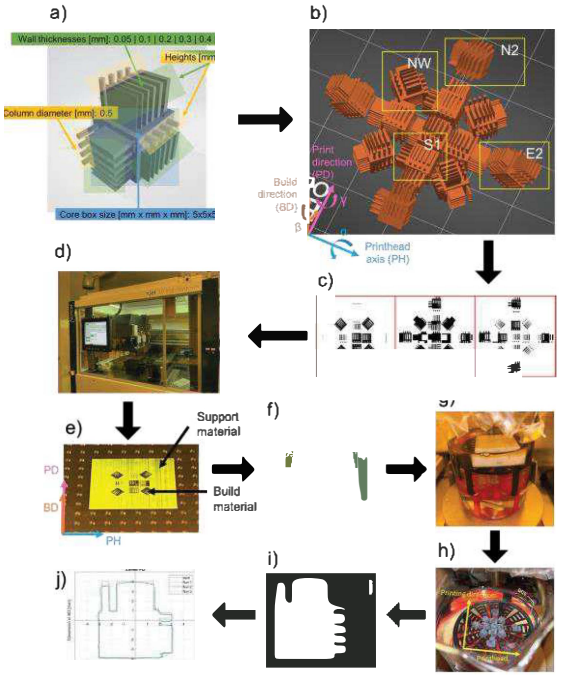

Fig. 1 Materials and methods deployed in this study

3. Results and Discussion

3.1. Contour plots of the printed specimens

Fig. 2a-d display the contour plots of the 13 printed specimens viewed from the print direction/build direction (PD/BD) (Fig. 2a, b) and printhead axis/build direction (PH/BD) plane (Fig. 2c, d). Each plot contains four data curves. The red curve depicts the ideal contour of the test specimen, while the remaining curves, labelled Run1 to Run3, represent the contours of the printed specimens that were printed three times. The position of each plot is denoted in the title according to the cardinal points. Fig. 2b and Fig. 2d depict the specimens that were rotated, and the x and y-axis specify the rotation angle, where applicable. For instance, the specimens positioned in NW, NE, SW, and SE are rotated around the BD-axis by 45° (rotational angle γ), whereas the specimens at N2 and W2 are rotated around the PH-axis (rotational angle α), and E2 and S2 around the PD-axis (rotational angle β). Additionally, the plots with the rotated specimens are accompanied by an image of the corresponding 3D model on the slicer platform, where the plane demonstrated in the plot is marked in green (PD/BD plane) or purple (PH/BD plane) to visualize the illustrated contours. Fig. 2a and c demonstrate the remaining specimens, with planes of interest that are equivalent to the side views of the specimens.

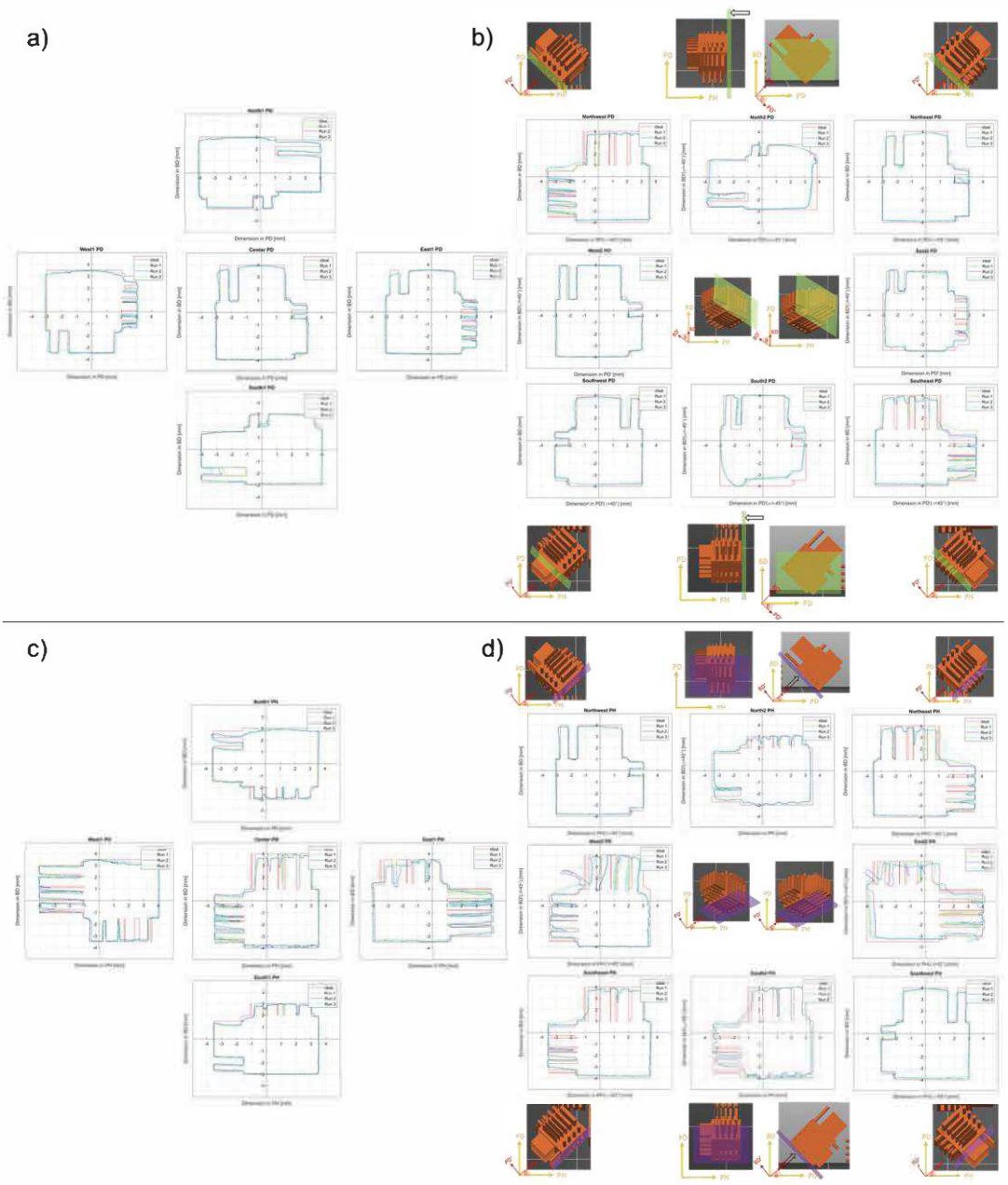

Fig. 2 Contours of the non-rotated printed specimens viewed from the PD/BD plane (a), rotated printed specimens viewed from the PD/BD plane (b), non-rotated printed specimens viewed from the PH/BD plane (c), rotated printed specimens viewed from the PH/BD plane (d)

3.1. Geometrical accuracy of the top horizontal edge

3.1.1 Print direction / Build direction plane

The plots shown in Fig. 4 illustrate the resulting shape of the horizontal edges of the printed specimens at various orientation and either viewed from the PD/BD or PH/BD plane. From this Figure, it can be concluded that the most accurate horizontal edges (quality level 5) are observed for the specimens placed on the outer area of the whole assembly, namely E2, S2, and W2 (except for N2), which are all rotated by 45° around the PD-axis or by -45° around the PH-axis (Fig. 4a). The reason why the specimen N2 does not possess an ideal top horizontal edge is due to the rotation and the fact that adjacent to this top horizontal edge, no support material is printed, resulting in a lack of side support (Fig. 3). Without support material, the build material will spread sideways, preventing the realization of sharp edges. S2 shows similar behavior for its lower horizontal edge (Fig. 2b), but it is not considered in the plots in Fig. 4 as only the top horizontal edge is assessed.

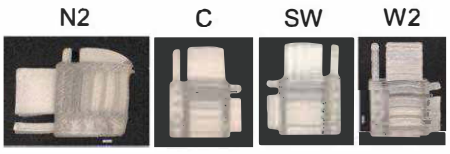

Fig. 3 Microscope images of specimens N2, C, SW, W2 viewed from the PD/BD plane

The remaining specimens shown in Fig. 4a are mainly exhibiting a slightly convex top horizontal edge. This behavior indicates that rotation around either the PD- or PH-axis improves the accuracy of horizontal edges compared to a specimen whose horizontal edge is parallel to the PD-axis (rotation around BD-axis). The improvement of the horizontal edge geometry observed for the rotated specimens could be explained as follows.

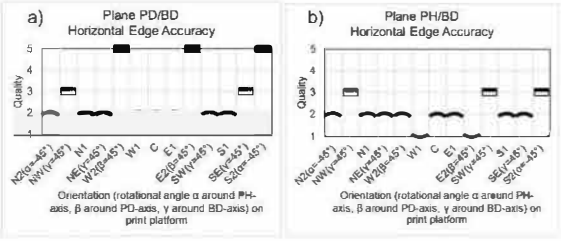

Fig. 4 Geometrical accuracy of the top horizontal edges of the test specimens viewed from the PD/BD (a) and PH/BD (b) side and rotated in different directions according to the given rotational angle (Quality criteria 1=concave, 2=convex, 3=below ideal shape, 4=exceeding ideal shape, 5=ideal shape)

For specimens rotated around the PH-axis, the horizontal edge is essentially generated by the outset droplets of the printed pattern in each layer (Fig. 5a). Moreover, due to the rotation by 45° around the PH- or PD-axis, the droplets are stacked on top of each other being slightly shifted. Hence, any droplet height differences are averaged through the printing process. For the other specimens rotated around BD-axis, on the contrary, the horizontal edge is essentially the accumulated surface profile of all printed layers (Fig. 5b).

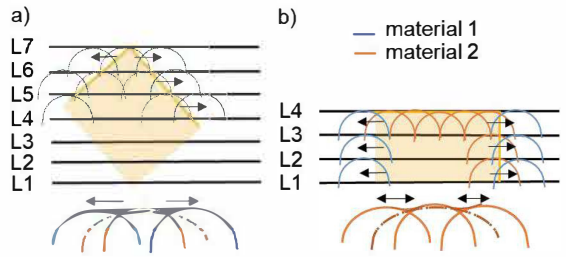

Fig. 5 Potential droplet coalescence scenario in this printing process

Considering that both materials, support and build material, are being printed simultaneously, the build material droplets seem to be drawn to the support material more strongly during the coalescence process, once they are deposited next to each other. As a result, build materials droplets adjacent to the support material area might be less in height compared to a droplet surrounded by the same material, the build material (Fig. 5). Consequently, this distinct convex shape is present for all structures in dependent of their position on the print platform but which horizontal edge is parallel to the printing plane.

The coalescence process of two droplets are governed by their physical properties regarding interfacial tension, droplet size [16] and viscosity [17]. For identical physical properties, the coalescence process of two droplets behaves in a rather symmetrical way, whereas any large difference in diameter or interfacial tension could accelerate the mixing and result in an asymmetrical process. For instances, for same-size droplets with different interfacial tension, the fluid of the droplet with the higher interfacial tension is transferred to the lower interfacial tension droplet. The convection of the liquid between two droplets with different sizes are directed from the smaller droplet to the larger one [16]. Lower viscosity of the larger droplet and higher viscous smaller droplet increases the mixing process as well [17].

Two of these three above-mentioned scenario could be applied to the printing process as both materials are dissimilar in their chemical formulation, hence the interfacial tension could potentially differ. Furthermore, due to the different viscosity, the print temperature of the build material is set to a higher level than the support material. This means, that the viscosity of the droplets upon the impact onto the substrate (at room temperature) is different as well, favoring asymmetrical coalescence behavior. The third condition regarding the dissimilar droplet size is not applicable to the contours visible on the PD/BD view as the contours are created from the same nozzle, therefore should not be subject to any droplet volume variations.

3.1.2 Printhead axis/ Build direction plane

The geometrical accuracy of the horizontal edge aligned parallel to the PH-axis (Fig. 4b) is subject to larger variations – from edges that are below the ideal shape (smaller) to curved edges, that can be either concave or convex.

The shapes do not occur in a regular manner, because it is induced by the droplet volume variation between individual nozzles within one printhead. Therefore, it can be observed that specimens that are printed with the same nozzles (specimens that are positioned along the same axis parallel to the PD are exhibiting similar defects, such it is the case for the specimens N1, C, and S1 (Fig. 6). These specimens are all similarly shaped, with the top horizontal edge of the core body being slightly convex and with a reduced height in particular on the left region of the top horizontal line (Fig. 2c).

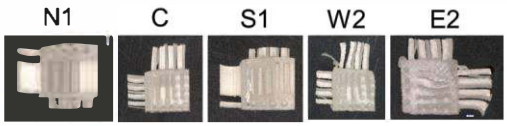

Fig. 6 Microscope images of specimens N1, C, S1, W2, E2 viewed from the PH/BD plane

The droplet volume variation is also visible in the central picture in Fig. 1f which depicts the printed object before dissolving the support material (white material). This particular not post-processed specimen presents traces in parallel to the printing direction on the surface, indicating either a reduction of droplet volume for some nozzles or non-firing ones. The droplet variation is particularly pronounced for the build material, which explains the high standard deviation for the average droplet volume, and which is also visible for the specimens N2 and S2. The base horizontal lines of these two specimens are rather irregular, as this line of build material droplets generated for the first layer represents the status of the utilized nozzle as no other build material droplet are existing around them and allowing any levelling of the

droplet height to the surrounding by merging with adjacent droplets of identical materials (Fig. 2d).

Overall, rotating the specimen around the PD-axis could barely improve the horizontal edge accuracy in parallel to the PH-axis, as the outcome depends on the variation of ejected droplet volume for each individual nozzle. Thus, while the horizontal edge of specimen W2 seems to be convex (Fig. 4b), the curvature of E2 is rather concave. The overall geometrical accuracy of these two specimens are also less than the other specimens due to the rotation around the print direction. In particular in Fig. 6 the partially collapsed slits in the core body of these two specimens point at a non-consistent layer height across the printhead axis (Fig. 6). In addition, the edges are less smooth which indicate a stair-case like surface as a result of the rotation [18]. The staircase effect takes place when the contour of the printed pattern between each layer shifts and the degree of change is large so that it affects the surface integrity.

3.1. Columns

Fig. 7 shows the result of the printed columns that are all printed successfully. However, within one specimen, variations of the columns' shape are present despite the identical design.

For instances, the vertical columns of the test specimen SW, viewed from the PH/BD plane (Fig. 7d), are either perfectly straight, or slightly tilted either to the right or to the left side.

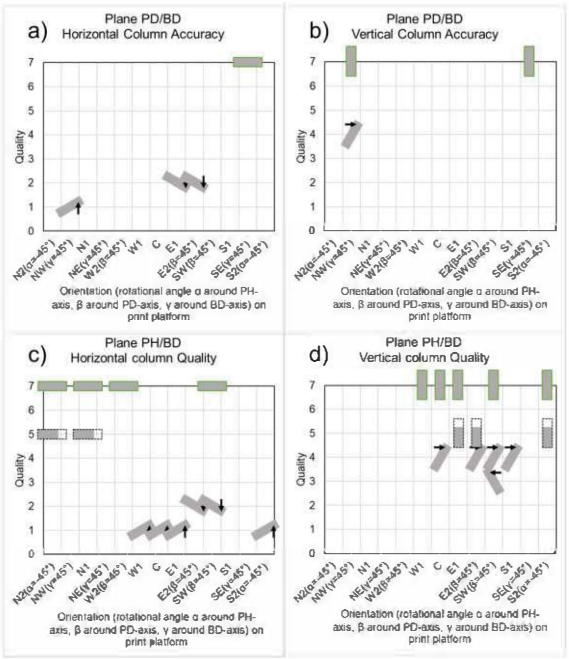

Fig. 7 Geometrical accuracy of the horizontal and vertical columns (all diameter 0.5 mm) of the test specimens viewed from the PD/BD (a,b) and PH/BD (c,d) plane (Quality criteria 1=tilted upwards, 2=tilted downwards, 3=tilted to the left, 4=tilted to the right, 5=shorter, 6=longer, 7=ideal shape)

The specimen E1 on the same view, on the other hand, exhibits columns that are shorter (Fig. 8). This variation could be caused by variations in the volume of the ejected droplet or the ejection trajectory. The latter explanation can be applied to the vertical columns viewed from the PD/BD plane as well.

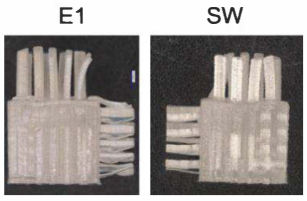

Fig. 8 Microscope images of specimens E1 and SW viewed from the PH/BD plane

The shapes of the horizontal columns (Fig. 7a,c), on the contrary, are rather consistent within one group of columns, since any tilting are governed by the droplet volume variation between individual nozzle at this particular position, and the ejected volume of one particular nozzles normally remains steady throughout the printing process since the same waveform is applied throughout all nozzles.

However, this explanation can only be applied to the horizontal structures generated in the direction of the PH-axis (e.g. specimens E1, SW, Fig. 8), whereas the features in the PD (e.g. NW, E1, Fig. 9) might be caused by a mismatch of droplet volume of both materials.

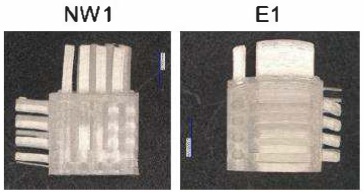

Fig. 9 Microscope images of specimens NW1 and E1 viewed from the PD/BD plane

If the support material of a particle nozzle generates smaller droplet volume than the build material, the layer height is reduced as well. Thus, the printed build material will be deposited on a lower level if printed on a layer of support material compared to when printed on a layer of build material. This scenario will cause a downward facing structure.

Fig. 10 Mismatch of layer height in multi-material printing leads to tilted columns or walls

3.2 Thin walls with varying aspect ratios

While Fig. 7 is showing the geometrical accuracy of a group of columns that are of same aspect ratio, the following Section presents the geometrical accuracy of the printed thin walls with aspect ratios ranging from 0.01 (50 µm width, 3 mm height) to 0.5 (500 µm width, 1 mm height). Since this study only assesses the specimens viewed from two particular views, not all examined views offered thin wall structures to be assessed which explains the "no data" boxes in Fig. 11 and Fig. 13.

The thinnest wall (50 µm width) collapsed for almost all specimens (Fig. 11, Fig. 13), however for

horizontal thin walls up to a length of 2 mm are well visible, but strongly tilted (Fig. 11).

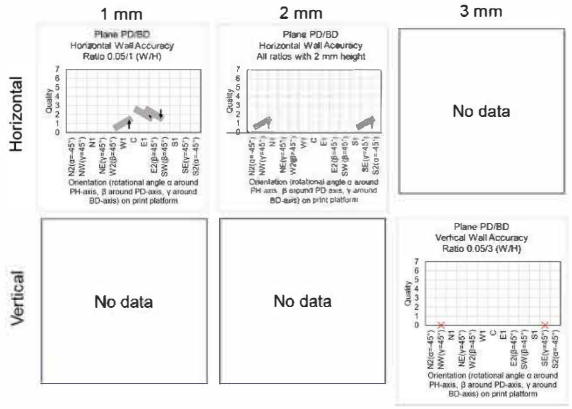

Fig. 11 Geometrical accuracy of the horizontal and vertical walls with 0.05 mm width and 1 mm to 3 mm lengths viewed from the PD/BD plane (Quality criteria 1=tilted upwards, 2=tilted downwards, 3=tilted to the left, 4=tilted to the right, 5=shorter, 6=longer, 7=ideal shape)

Fig. 12 depicts such a collapsed vertical thin wall (aspect ratio 0.01), whereas the horizontal thin wall with aspect ratio 0.02, i.e. 2 mm length, is tilted.

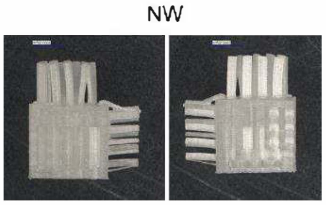

Fig. 12 Test specimen on position NW viewed from (left) and on (right) the PD/BD plane with both horizontal (length 2 mm) and vertical thin walls (length 3 mm)

With regards to the structures visible from the PH/BD view, most specimens exhibit collapsing thin walls or strongly tilted walls (Fig. 13). The direction of tilting for all thin walls are arbitrary, which suggests that a structure with this width can barely support itself if printed with this particular material and printing condition (Fig. 14).

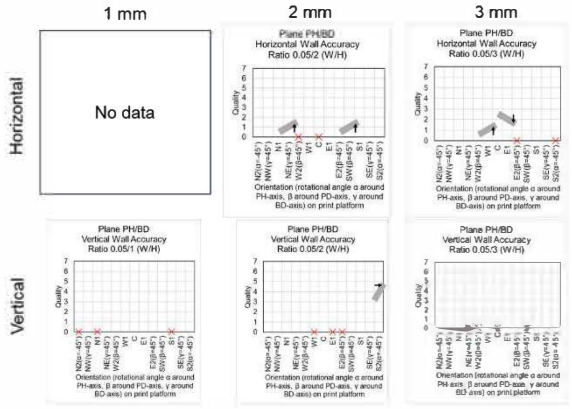

Fig. 13 Geometrical accuracy of the horizontal and vertical walls with 0.05 mm width and 1 mm to 3 mm lengths viewed from the PH/BD plane (Quality criteria 1=tilted upwards, 2=tilted downwards, 3=tilted to the left, 4=tilted to the right, 5=shorter, 6=longer, 7=ideal shape)

Furthermore, the flowing motion induced by the magnetic stirrer during the dissolvement process of the support material might exert small forces on the thin structures, provoking a collapse or tilting of the thin walls. In addition, swelling of the printed structure due to the immersion in the solvent for several hours could happen which would come with a reduction of the stiffness of the printed structure, thus is more likely to give in if exposed to any forces.

For all other aspect ratios, the walls are present, although tilting still exists for some of them. The reasons for the arbitrary tilting must be similar to what has already been described for the columns. As a general rule of thumb, the likelihood of a structure to collapse is lower for horizontally thin walls and for an aspect ratio greater than 0.2 (0.1 mm width, 3 mm length) all thin structures could be printed, but might be tilted (for lengths 2 mm and greater).

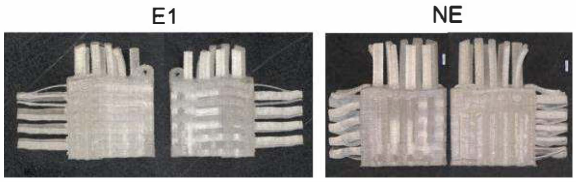

Fig. 14 Test specimens on position E1 and NE viewed from (left) and on (right) the PH/BD plane with both horizontal (2 and 3 mm lengths) and vertical thin walls (2 and 3 mm lengths)

4. Conclusion

The objective of this study is to examine the influence of placement orientation of the 3D object on the geometrical accuracy of the printed microfeatures. Three properties are assessed qualitatively: the horizontal and vertical edges, the columns, and the thin walls. The main findings of this study are as follows.

- Horizontal edges are most accurate if the specimen is rotated either around the print direction or the printhead axis (in this study, the rotation angle is 45°).
- The droplet coalescence of two different materials, e.g., support material and build material, can lead to an asymmetrical merging process and result in slightly different heights compared to merging between droplets of identical properties. This difference affects the dimensional quality of the top horizontal edge, especially if it is printed parallel to the printing plane.
- Edges that are not supported with support material on one side are subject to spreading, thus compromising geometrical accuracy.
- The columns of consistent diameter (0.5 mm) are all printed successfully, although some are tilted. Several reasons can cause this geometrical inaccuracy, such as droplet variation between nozzles, skewed trajectory of the printed droplet (applicable to vertical columns and horizontal columns parallel to the printhead axis), or a difference in layer height of both materials

(particularly for horizontal columns printed in the print direction).

- Thin wall structures with a width of 50 µm are susceptible to collapse after the removal of the support material. Vertical thin walls are more likely to collapse compared to horizontal thin walls of the same size viewed from the same plane.

This qualitative assessment of the printed specimen with microfeatures below 1 mm in width, printed with different orientations (rotated by either 45° or 90°), provides insight into the numerous factors that influence geometrical accuracy.

Since this study only assessed the quality from two perspectives, the plane print direction/build direction and printhead axis/build direction, it is suggested to extend the assessment to all six faces of the specimen to obtain a complete picture of the effect of print orientation on microfeatures of all sizes and aspect ratios. The specimen used in this study also contains negative features (slits and holes) that have not been investigated in this paper but should be examined in the future. Furthermore, the influence of the support material removal on the material's mechanical properties should be examined, as it could limit the possible aspect ratio of the printed part (if swelling and, therefore, reduction of stiffness occurs).

Generally, support material consumption made up a large portion of this printing process. Hence, from a sustainability point of view, studying smart support material distribution to achieve the least amount of waste material (support material is considered waste material as it is dissolved after the printing process) while ensuring the highest geometrical accuracy is essential. This study concluded that the accuracy of vertical edges without support material is substantially reduced.

A close control of the droplet coalescence behavior of two droplets with different viscosity and physical properties, as in the case for the interface region between two materials, is crucial to obtain high precision of the printed object and ought to be investigated. Rotation around the print direction or printhead axis results in a staircase effect on the surface. Knowing the correlation between the thickness of the layer, the degree of contour shift, the rotation angle, and the resulting surface roughness would provide a useful tool for future operators to choose the rotation angle according to the desired surface integrity.

Many observed defects are assumed to be caused by inaccuracies in the printing process itself, such as droplet diameter variation and skewed droplet trajectory. Ensuring identical layer height when printing multi-material is very challenging, as minor differences in the range of one-tenth of microns can accumulate to a few dozen microns after several hundred layers. To combat these printhead-induced factors, efforts should be made to develop droplet quality optimization methods, either before the printing or during the printing process.

Acknowledgements

This work was carried out with the support of the Karlsruhe Nano Micro Facility (KNMFi, www.knmf.kit.edu) a Helmholtz Research Infrastructure at Karlsruhe Institute of Technology (KIT, www.kit.edu) and under the Helmholtz Research Programme MSE (Materials Systems Engineering) at KIT. The authors thank BASF Forward for providing us with the build and support material.

References

[1] A. Elkaseer et al., "Effect of Process Parameters on the Performance of Drop-On-Demand 3D Inkjet Printing: Geometrical-Based Modeling and Experimental Validation," *Polymers,* vol. 14, no. 13, 2022.

[2] A. Muguruza et al., "Development of a multi-material additive manufacturing process for electronic devices," *Procedia Manufacturing,* vol. 13, pp. 746–753, 2017.

[3] S. Schlatter et al., "Inkjet Printing of Complex Soft Machines with Densely Integrated Electrostatic Actuators," *Advanced Intelligent Systems,* vol. 2, no. 11, 2020.

[4] A. Lion et al., "Customisable Tablet Printing: The Development of Multimaterial Hot Melt Inkjet 3D Printing to Produce Complex and Personalised Dosage Forms," *Pharmaceutics,* vol. 13, no. 10, Oct 14, 2021.

[5] T. J. K. Buchner et al., "Vision-controlled jetting for composite systems and robots," *Nature,* vol. 623, no. 7987, pp. 522-530, 2023.

[6] L. B. Bezek et al., "Mechanical properties of tissue-mimicking composites formed by material jetting additive manufacturing," *Journal of the mechanical behavior of biomedical materials,* vol. 125, pp. 104938, 2022.

[7] A. Elkaseer et al., "Material jetting for advanced applications: A state-of-the-art review, gaps and future directions," *Additive Manufacturing,* vol. 60, pp. 103270, 2022.

[8] K. J. Chen et al., "A study on the effect of process parameters on feature resolution in 3D inkjet printing," in World Congress on Micro and Nano Manufacturing, Evanston, USA, 2023.

[9] K.-E. Aslani et al., "Surface Roughness Optimization of Poly-Jet 3D Printing Using Grey Taguchi Method," *2019 International Conference on Control, Artificial Intelligence, Robotics & Optimization (ICCAIRO)*, pp. 213–218: IEEE, 2019.

[10] L. Zorzetto et al., "Properties and role of interfaces in multimaterial 3D printed composites," *Scientific reports,* vol. 10, no. 1, pp. 22285, 2020.

[11] I. Q. Vu et al., "Characterizing the effect of print orientation on interface integrity of multi-material jetting additive manufacturing," *Additive Manufacturing,* vol. 22, pp. 447–461, 2018.

[12] N. Majca-Nowak et al., "The Analysis of Mechanical Properties and Geometric Accuracy in Specimens Printed in Material Jetting Technology," *Materials (Basel),* vol. 16, no. 8, 2023.

[13] A. Khoshkhoo et al., "Effect of build orientation and part thickness on dimensional distortion in material jetting processes," *Rapid Prototyping Journal,* vol. 24, no. 9, pp.

1563-1571, 2018.

[14] M. R. Silva et al., “Assessment of the Dimensional and Geometric Precision of Micro-Details Produced by Material Jetting,” *Materials (Basel),* vol. 14, no. 8, Apr 15, 2021.

[15] A. Elkaseer et al., “On the quantitative assessment of the effect of multiple process parameters on the printed layer height in 3D inkjet printing,” *Virtual and Physical Prototyping,* vol. 18, no. 1, 2023.

[16] X. Luo et al., “Mixing characteristics and energy conversion in the coalescence process of the two droplets,” *Chemical Engineering Science,* vol. 248, 2022.

[17] V. S. Akella et al., “Universal scaling laws in droplet coalescence: A dissipative particle dynamics study,” *Chemical Physics Letters,* vol. 758, 2020.

[18] S. Sikder et al., “Effect of Adaptive Slicing on Surface Integrity in Additive Manufacturing,” in 34th Computers and Information in Engineering Conference, Buffalo, USA, 2014.